Opposite Effects of Electrostatics and Steric Exclusion on Bundle Formation by F-Actin and Other Filamentous Polyelectrolytes†

Jay X. Tang,*,‡ Tadanao Ito,§ Terence Tao,|| Peter Traub,⊥ and Paul A. Janmey‡

Division of Experimental Medicine, Brigham and Women's Hospital, Program in Biological and Biomedical Sciences, Harvard Medical School, 221 Longwood Avenue, LMRC 301, Boston, Massachusetts 02115, Department of Biophysics, Kyoto University School of Science, Kyoto 606-01, Japan, Muscle Research Group, Boston Biomedical Research Institute, 20 Staniford Street, Boston, Massachusetts 02114, and Max Planck Institute for Cell Biology, Ladenburg bei Heidelberg, Germany

Received May 15, 1997; Revised Manuscript Received July 31, 1997⊗

ABSTRACT: A number of positively charged polypeptides and proteins bundle DNA, F-actin, microtubules, and viruses such as filamentous phage fd and tobacco mosaic virus (TMV), as well as intermediate filaments formed by vimentin. The general behavior is dictated by the common polyelectrolyte nature of these biopolymers, which gives rise to nonspecific binding by ligands carrying several net opposite charges. An attractive interaction accounts for the subsequent lateral aggregation, distinguishing this transition from the liquid crystalline formation of filamentous particles at high concentrations. Morphologically similar filament bundles can also be induced by inert solutes such as polyethylene glycol (PEG) and proteins that do not bind the macromolecular filaments, but the physicochemistry underlying this class of bundle transitions is distinct. In particular, bundling transitions induced by electrostatic and steric mechanisms have an opposite dependence on the solution ionic strength and the concentration of the filamentous biopolymers. The distinct mechanisms illustrated in this report may each contribute to the formation of specific polymer bundles under physiological conditions.

Bundles and condensed tangles of filamentous polymers are common in cells and biological tissues, ranging from the apparently amorphous chromatin condensed in the nucleus to the paracrystalline arrays of actin filaments in stress fibers, microvilli, and filopods (*1*). The formation of such structures is generally orchestrated by the activity of specific ligands, including many proteins, but the general thermodynamic driving force of their formation, except for the case of DNA (*2*, *3*), has not received broad attention.

DNA condensation is a well-known phenomenon and has been explained theoretically on the basis of the concept of counterion condensation (*4*, *5*). The process requires a threshold concentration of polyvalent cations such as polyamines to enhance the extent of charge neutralization. The force balance includes a screened electrostatic repulsion between the charged DNA molecules and attractive interactions due primarily to the fluctuation (*5*) and lateral redistribution (*6*) of counterions. The van der Waals force and the effects of hydration (*2*, *3*, *7*−*9*) may also contribute to the overall equilibrium association of either rodlike or toroidal DNA superstructures.

Recently, a behavior similar to DNA condensation has been shown with other charged, filamentous biological assemblies, including the cytoskeletal filaments F-actin and microtubules (*10*, *11*). Bundles of F-actin can be induced by divalent metal ions, trivalent cations such as cobalt hexamine, oligomers of positively charged amino acids, and proteins with highly positively charged domains. Due to the simple geometric constraint and the stiffness of the filament, the lateral association of F-actin in the condensed phase gives rise to a paracrystalline packing. The morphology of actin paracrystals has been extensively characterized by electron microscopy techniques (*12*−*16*). Although in some cases distinct packing arrangements occur due to specific bonding of certain bundling agents (*15*, *17*), the general features agree well with the predictions based on the polyelectrolyte nature of F-actin.

Many types of biomolecular filaments, including DNA, are anionic with linear charge densities sufficiently high to stabilize electrostatic interactions with polycations even at physiological ionic strengths. This important class of biopolymers includes F-actin, microtubules, intermediate filaments, and some filamentous viruses. Theories of polyelectrolytes developed to account for cation-induced condensation of DNA can be applied to these protein filaments, providing an explanation for the ability of many specific polycationic proteins to be efficient bundling factors for some or all of these diverse filament types. In this general model, the binding of these different cationic proteins to the different filamentous substrates is the predicted prerequisite for bundling. However, the actual binding sites between the cationic proteins and the different filamentous substrates may vary greatly. The variation is closely correlated with the conformations and electrostatic potential profiles of both the protein ligand and the substrate filament.

In this paper, we limit our focus to some of the general features of bundle formation induced by certain cationic proteins or polypeptides. We demonstrate that this class of

† This work is supported by National Institutes of Health (NIH) Training Grant HL19429 and NIH Grant AR38910 to P.A.J., P01-AR41637 to T.T., and Cystic Fibrosis Foundation Grant G957 to P.A.J.

* Address correspondence to Jay X. Tang, Division of Experimental Medicine, Brigham and Women's Hospital, 221 Longwood Ave., LMRC 301, Boston, MA 02115. Telephone: 617 278-0388. Fax: 617 734-2248. E-mail: tang@calvin.bwh.harvard.edu.

‡ Harvard Medical School.

§ Kyoto University School of Science.

|| Boston Biomedical Research Institute.

⊥ Max Planck Institute for Cell Biology.

⊗ Abstract published in *Advance ACS Abstracts,* September 15, 1997.

S0006-2960(97)01138-0 CCC: $14.00

bundle formation is unrelated to the isotropic to liquid crystal transition of F-actin at high concentrations (*18*−*21*). We also show the differences between the polycation-mediated bundle formation and that of morphologically similar ordered arrays of actin caused by addition of inert macromolecules such as polyethylene glycol (PEG)[1] (*22*).

MATERIALS AND METHODS

Proteins. Monomeric actin was prepared from an acetone powder of rabbit skeletal muscle according to Spudich and Watt (*23*). The nonpolymerizing actin solution contained 4 mM Hepes buffer at pH 7.2, 0.2 mM $CaCl_2$, 0.5 mM ATP, 0.2 mM DTT, and 0.5 mM NaN_3. Actin was polymerized by 2 mM $MgCl_2$ and 150 mM KCl, unless otherwise noted.

Recombinant chicken gizzard α-calponin (CaP) was produced as described in Gong et al. (*24*), and the protein was handled in the manner described earlier (*11*). Tubulin was purified using the method of Voter and Erickson (*25*), and the preparation of paclitaxel-stabilized microtubules for light scattering experiments was described previously (*10*). Vimentin was purified by a published method (*26*), and the vimentin intermediate filaments were formed by bringing the salt concentration to 150 mM KCl prior to the bundling experiments.

Calf thymus histone (H1) was purchased from Sigma (St. Louis, MO), classified therein as type III-S. Lysozyme from chicken egg white was supplied by ICN Pharmaceuticals (Irvine, CA). Both proteins were used without further purification. A stock solution of each protein was prepared at a concentration of 200 μM, dissolved in a buffer solution of 10 mM Hepes at pH 7.5.

Peptides and DNA. The myristoylated alanine-rich protein kinase C substrate (MARCKS) peptide was purchased from Biomol (Plymouth Meeting, PA), supplied as the trifluoroacetate salt. Polylysines with average degrees of polymerization of 18 and 42 were both purchased from Sigma. For each peptide, a stock solution of 200 μM was prepared in 50 mM Hepes at pH 7.5 prior to additions into F-actin solutions. DNA from salmon testes was purchased from Sigma.

Viruses. Tobacco mosaic virus (TMV) was purified in the lab of D. L. D. Caspar at the Rosenstiel Basic Medical Research Center of Brandeis University (*27*). Filamentous phage fd was prepared in the same lab by a standard method (*28*). Both virus suspensions were kept in 2 mM Tris at pH 7.5 and 0.5 mM NaN_3. Concentrations of the virus suspensions were determined by optical absorbance. The following specific absorbances were used: 3.84 mL mg^{-1} cm^{-1} at 269 nm for fd and 3.05 mL mg^{-1} cm^{-1} at 280 nm for TMV.

Light Scattering Measurements. Ninety degree light scattering measurements were performed using a Perkin-Elmer LS-5B luminescence spectrometer (*11*). The wavelength setting was 365 nm for the incident beam and 370 nm for detection of scattered light. Whenever intensities were compared among different samples, the slits for both beams were fixed at 3 nm.

Polarization Photometry. A handmade light box was used to observe the concentrated F-actin samples. Two polarization sheets, purchased from Polaroid Corp. (Cambridge, MA), were added in the optical path in order to observe the birefringent domains. The sample held in a glass tube with a 6 mm diameter was immersed in water to achieve an approximate refractive index match. The optical images were taken by a Contax camera, using a Zeiss lens with a 60 mm focal length (Carl Zeiss, model 7073234).

Centrifugation Assay. The fraction of F-actin in the PEG-induced bundles was determined by the low-speed centrifugation method as described previously (*22*).

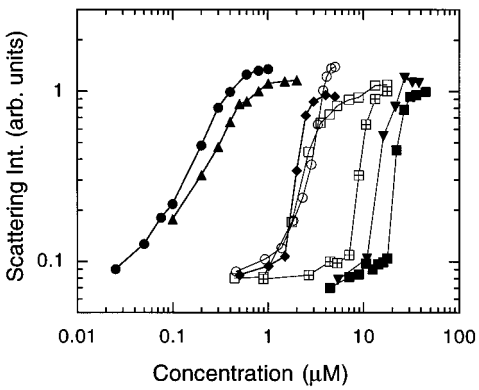

FIGURE 1: Light scattering detection of bundle formation of 0.2 mg/mL F-actin following sequential additions of histone H1 (filled circles), Lys_{42} (up triangles), Lys_{18} (down triangles), MARCKS peptide (diamonds), smooth muscle calponin (empty circles), and lysozyme (any squares). The F-actin solution initially contained 2 mM $MgCl_2$ and 50 (open symbols), 100 (crossed squares), or 150 mM KCl (solid symbols). The data in squares for lysozyme at the three KCl concentrations show that bundle formation at a higher ionic strength requires an increased amount of lysozyme, a property shared by all the cationic bundling agents.

RESULTS

Cationic Proteins and Basic Polypeptides Bundle F-Actin. We have recently proposed a mechanism of actin bundle formation based on the polyelectrolyte nature of F-actin and the condensation of polyvalent cations which consequently induce lateral aggregation (*11*). In this work, we begin by demonstrating that several genetically unrelated cationic proteins can induce the formation of actin bundles, and comparing their bundling efficiency with that of polylysines with known degrees of polymerization. Figure 1 demonstrates the formation of actin bundles using light scattering to detect lateral aggregation of the filaments. A sharp increase in the scattering intensity indicates formation of large aggregates. Substoichiometric amounts of the highly basic protein histone (H1) efficiently cross-link and bundle F-actin. A slightly higher molar concentration of a synthetic polylysine with an average degree of polymerization of 42, Lys_{42}, is required to bundle an equal concentration of F-actin. Polylysine at more than 10 μM with a lower degree of polymerization, Lys_{18}, was required to induce the bundle formation of F-actin. A 25-amino acid, highly basic polypeptide hypothesized to be the specific actin binding domain of the MARCKS protein also bundles F-actin at micromolar concentrations. Intact proteins such as chicken smooth muscle calponin and egg white lysozyme also bundle F-actin with comparable affinities.

If the bundling activity of the diverse factors shown in Figure 1 is primarily due to the polyelectrolyte nature of

[1] Abbreviations: MT, microtubule; VI, vimentin; TMV, tobacco mosaic virus; PEG, polyethylene glycol; DTT, dithiothreitol; CaP, calponin; MARCKS, myristoylated alanine-rich protein kinase C substrate.

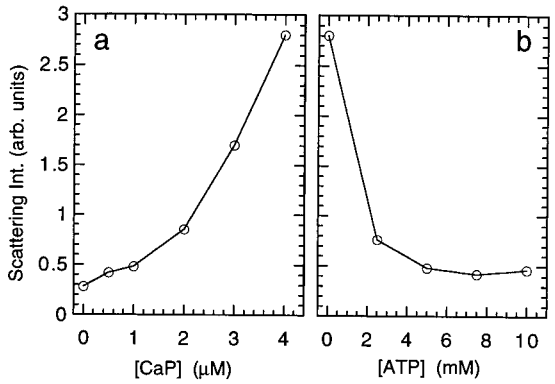

FIGURE 2: Reversible aggregation of vimentin intermediate filaments by smooth muscle calponin (CaP). (a) Bundle formation of 0.5 mg/mL vimentin induced by CaP. Vimentin filaments were polymerized by 150 mM KCl prior to sequential additions of CaP. (b) Disaggregation of CaP (4 μM)−vimentin bundles by ATP.

F-actin, then bundle formation would require increasing concentrations of the basic proteins in solutions of increasing monovalent ions. This general property is due to competition between the charged ligands and small cations, while a threshold fraction of the polyvalent cations is necessary for the bundling to occur (*4*). A typical range of variation is shown with lysozyme at three salt concentrations of 50, 100, and 150 mM KCl in the F-actin solution (Figure 1, square symbols).

Smooth Muscle Calponin Induces Aggregation of Vimentin Intermediate Filaments. A few recent studies have shown that different cytoskeletal filaments are interconnected in cells (*29*, *30*), at least in some cases by proteins that are capable of cross-linking different filament types (*30*). The general mechanism of actin bundle formation, illustrated in Figure 1, leads to the suggestion that some cationic proteins may function as cross-linkers of different polyanionic cytoskeletal filaments. Microtubule-associated proteins such as MAP2 and tau have been shown not only to bind and bundle F-actin (*31*) but also to induce heterologous bundles of both microtubules and F-actin in vitro (*32*). This effect is likely due to the cationic nature of both proteins. Here, we test if calponin, a cationic protein which is associated with the smooth muscle thin filaments, is also capable of interacting with vimentin intermediate filaments.

Figure 2a shows the increase in scattering intensity following sequential additions of calponin into 0.5 mg/mL vimentin. The initial intensity corresponds to the scattering from dispersed vimentin filaments, previously formed at physiologic ionic strengths. Figure 2b shows that the formation of vimentin bundles can be reversed by adding ATP. Such a phenomenon has been reported to occur with calponin-induced actin bundles (*33*, *34*). Therefore, this property is not specific for vimentin, but rather, it suggests strongly that the polyanionic ATP competes against vimentin filaments for binding to calponin and hence inactivates the bundling ability of calponin.

Polylysine Bundles Six Unrelated Types of Anionic Filamentous Biopolymers. The bundling of different filamentous biopolymers is compared in Figure 3 using Lys_{18} as a representative bundling agent. Prior to addition of Lys_{18}, the scattering of equal weight concentrations of each biopolymer is compared in Figure 3a. Note the depicted stepwise increase in scattering intensity correlates with a

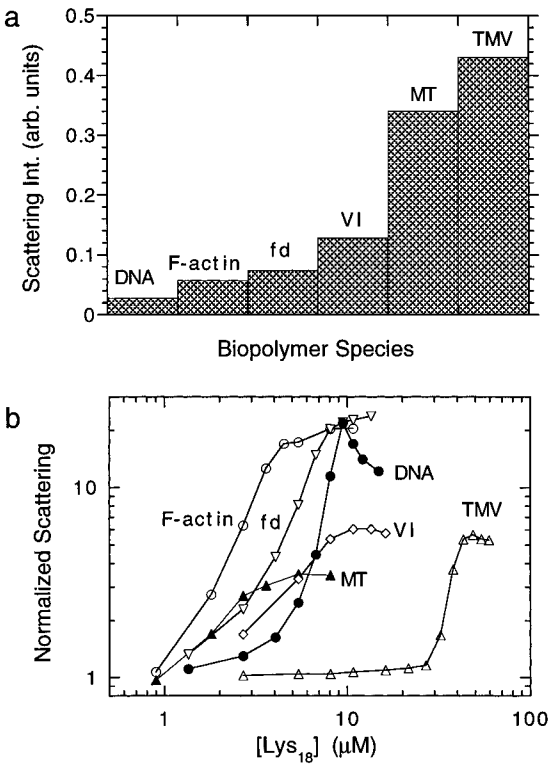

FIGURE 3: (a) Comparison of scattering intensity of various biopolymers prior to the bundling experiment. (b) The normalized scattering increase caused by sequential additions of Lys_{18}. The weight concentration of each biopolymer is 0.2 mg/mL, and the ionic strength is between 50 and 60 mM for all solutions.

sequential increase in the filament diameter, except that the diameter of TMV (18 nm) is notably smaller than that of a microtubule (25 nm). Since the average filament length of each measured species is at least comparable with the wavelength of scattering light (365 nm), the light scattering generally becomes insensitive to the filament length. In the cases of F-actin and MT, however, fractions of each protein exist in the forms of monomers, oligomers, and short fragments. This may explain why MTs scatter less than TMV even though the diameter of TMV is smaller than that of MT, and why F-actin scatters less than fd with a comparable filament diameter. The higher refractive index of polynucleotides compared to that of proteins may also account for the finding that the viruses scatter more light than the pure protein filaments with comparable diameters.

Figure 3b compares the increase in scattering intensity as the concentrated stock solution of Lys_{18} was added in sequential steps. Highly scattering aggregates were induced in all samples, but different filaments required different concentrations of Lys_{18} to aggregate. Such differences in the onset of filament bundling are related to the linear charge density of the filaments, with the more highly charged filament being more resistant to aggregation. For instance, F-actin with a charge of roughly 4 e/nm (*11*) is more susceptible to bundling than the fd virus with roughly 10 e/nm at pH 7.5 (*35*). Since many other factors, including the filament diameter, also strongly affect the aggregation, there is no simple rule in predicting the bundling threshold among the filaments of different species. The relative increase in scattering is less drastic for the species with large diameters and thus larger initial scattering. Therefore, the magnitude of the scattering increase appears to be dependent

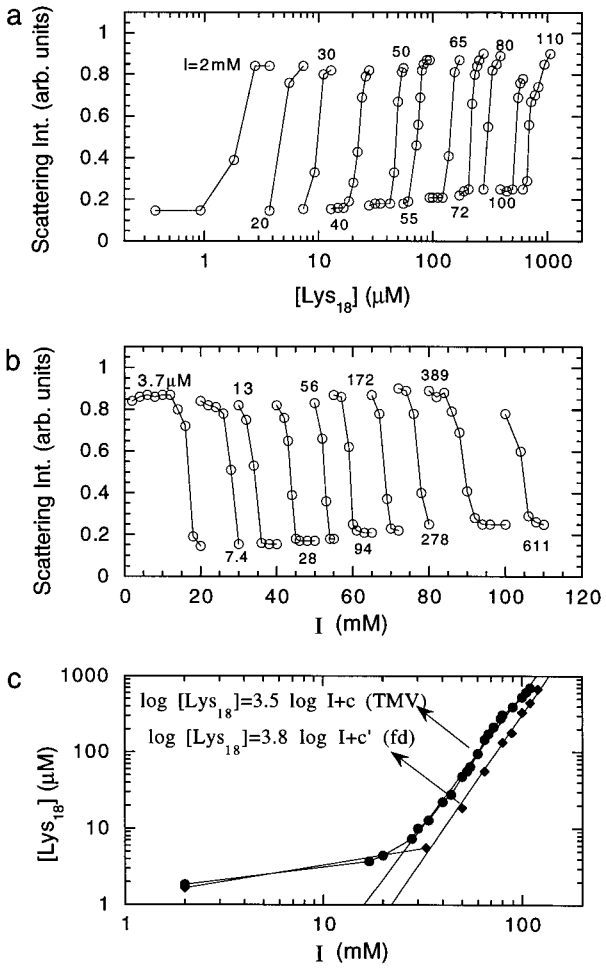

FIGURE 4: TMV (0.1 mg/mL) in a solution with an ionic strength of 2 mM was first subjected to sequential additions of a concentrated stock solution of Lys_{18} until the scattering saturated at a high level (a), followed by additions of concentrated KCl in sequential steps until the highly scattering bundles were dispersed (b). This process was repeated for a total of 10 cycles, divided into curves each corresponding to a set of measurements at either a fixed ionic strength (a) or a fixed concentration of Lys_{18} (b). (c) Relationship between [Lys_{18}] and the solution ionic strength as determined from panels a and b. A power law fit was applied where $I > 25$ mM, and the slope is shown for both TMV and fd.

on the diameters of respective filaments, but the common features in Figure 3b demonstrate a rather general behavior of this class of interfilament associations.

A Quantitative Comparison of the Ionic Strength Dependence of fd and TMV Bundles Induced by Polylysine. The effect of ionic strength on the bundling process was studied quantitatively with suspensions of fd and TMV, since both viruses are extremely stable in a wide range of salt concentrations but differ strongly in filament diameter and surface structure. Figure 4 shows the sensitivity and reversibility of the bundle formation as a function of ionic strength. First, 0.1 mg/mL TMV in a low-salt solution with an ionic strength of approximately 2 mM[2] was induced to bundle by adding Lys_{18} to above 1 μM, shown as the first curve from the left in Figure 4a. When the scattering signal had reached saturation, indicating complete formation of bundles, a concentrated solution of KCl was sequentially added to the suspension until the bundles disaggregated, shown as the first curve from the left in Figure 4b. After the TMV particles were dispersed from the bundles, adding more concentrated Lys_{18} induced the aggregation again, shown as the second curve in Figure 4a. Such an operation has been repeated through many cycles, demonstrating the reversibility and salt dependence of this process.

The sharp changes in the scattering signal as a function of the added Lys_{18} and the ionic strength I, the sum of the initial ionic strength and the KCl concentration, define a relationship between [Lys_{18}] and I at which the solution goes through a sharp transition. The transition is between a state in which all the charged filaments are dispersed and one in which the filaments spontaneously aggregate laterally. Such a transition can be explained by a balance of forces. If one assumes that a fixed fraction of charge is neutralized when the balance is reached, the original treatment of Manning predicts a power law relationship between [Lys_{18}] and I that is independent of the nature of the aggregating filaments. Panel c of Figure 4 shows the dependence extracted from panels a and b of Figure 4 in the case of TMV, and a similar set of experiments for a 0.1 mg/mL fd suspension (*10*). In the ionic strength range between 30 and 100 mM, the experimental relationship between [Lys_{18}] and I obeys rather well a power law, with the same slope within the range of experimental error for the two completely different filament types. The slope value of roughly 3.6 falls between 1 and 18, in the range predicted by Manning's simplified one-variable treatment (*4*, *10*, *11*).

Note in Figure 4c that [Lys_{18}] is the concentration of total added Lys_{18}, while the power law relationship should only hold for the free Lys_{18} in solution. The fraction of Lys_{18} which is bound to the filaments is in the micromolar range and is negligible only at high ionic strengths when the total [Lys_{18}] is very high. In the low-salt limit, however, the bound fraction of Lys_{18} is comparable to or even larger than the amount of free Lys_{18} predicted by the power law relationship. Therefore, the plots in Figure 4c show that the total [Lys_{18}] required to bundle both viruses appears to deviate from the power law fit under low-salt conditions.

Distinction between the Cation-Induced F-Actin Bundles and the Liquid Crystalline State of F-Actin. The paracrystalline bundles of F-actin induced by polyvalent cations differ fundamentally from the liquid crystalline state of F-actin. A nematic liquid crystalline state of F-actin forms at above 2 mg/mL (*18*−*22*), and the isotropic−nematic transition can be quantitatively predicted with a statistical mechanical treatment following the initial formulation by Onsager (*36*−*38*). The steric interaction between the otherwise freely moving actin filaments due to the excluded volume effect predicts that the isotropic−nematic transition concentration is inversely proportional to the average filament length and is measured to be about 6 mg/mL for F-actin with a 1.4 μm average filament length (*21*). The theoretical prediction takes into account the effect of filament charge by introducing an effective diameter and a twist parameter (*39*). No attractive interaction is required for the formation of the liquid crystalline phase.

The formation of stable F-actin bundles requires the presence of polycations. It occurs at any concentration of F-actin, and the condition for the onset of formation is nearly independent of the filament length above an average value on the order of 100 nm (*11*). All these properties are in

[2] The solution contained 2 mM Tris-HCl at pH 7.5 and 0.5 mM NaN_3. The ionic strength is estimated by assuming 80% ionization of Tris and complete dissociation of NaN_3.

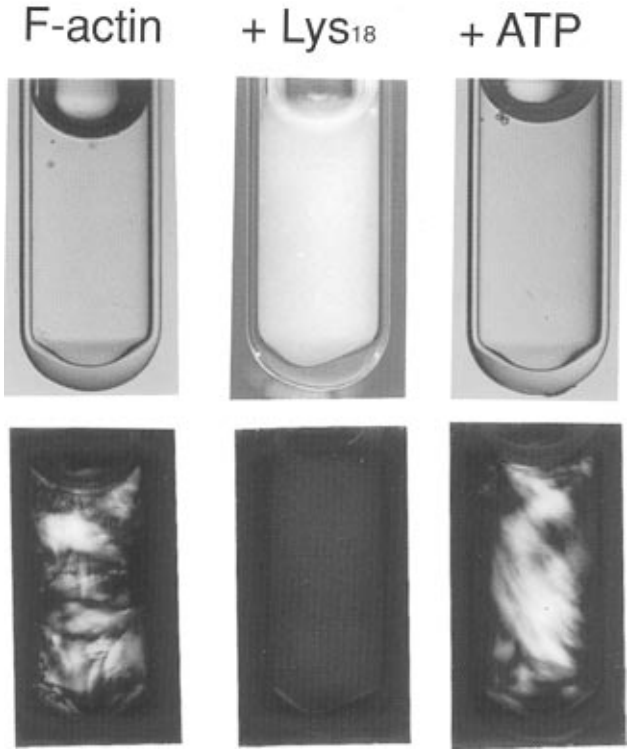

FIGURE 5: F-Actin (6.3 mg/mL) in a glass test tube was viewed without (upper panels) and with (bottom panels) crossed polarizers. The test tube is 6 mm in diameter and was immersed under water between two glass plates of a handmade cell to achieve an approximate refractive index match. Pictures were taken prior to addition of Lys_{18} (left) and after adding Lys_{18} to 50 μM (middle) and then after adding ATP to 10 mM (right). F-Actin was initially in a nematic liquid crystalline phase which is evident by the birefringence pattern through a set of crossed polarizers (bottom row, left) and formed highly scattering but nonbirefringent bundles after addition of 50 μM Lys_{18}. The bundles disassembled, and the liquid crystalline order was restored after adding ATP to 10 mM.

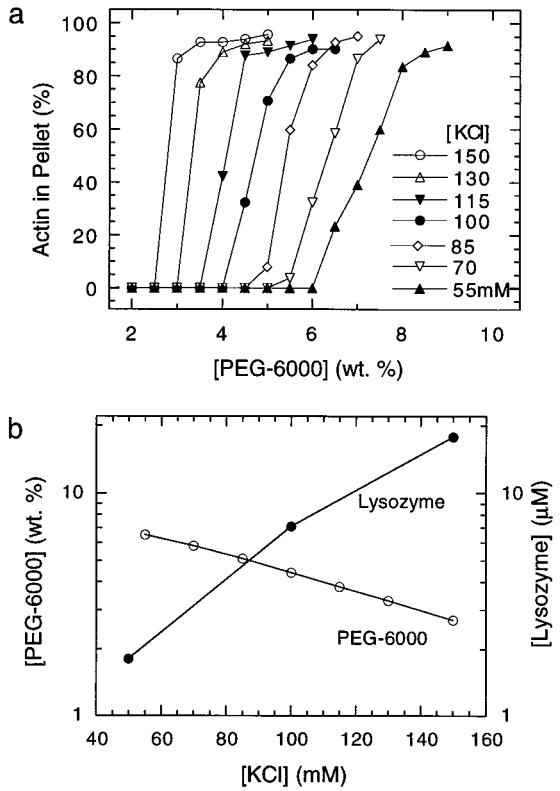

FIGURE 6: Low-speed sedimentation assay of actin bundles induced by PEG-6000 at various concentrations. (a) Percentage of F-actin sedimented by low-speed centrifugation as a function of the amount of PEG-6000 added. (b) Concentration of either the basic protein lysozyme or the inert PEG-6000 required to cause a noticeable formation of actin bundles as a function of solution ionic strength. F-Actin at a higher ionic strength requires more cationic agent but less PEG-6000 to facilitate bundle formation.

clear contrast to the formation of the liquid crystalline phase of F-actin as discussed above.

Figure 5 shows a visual comparison of the two distinct states described above. A 6.3 mg/mL F-actin sample in 2 mM $MgCl_2$ and 150 mM KCl was examined without (top panels) and with (bottom panels) crossed polarizers whose polarization axes are 45° off the vertical direction from each side. Birefringence patterns of millimeter scale indicated large nematic domains, which are aligned along a few random directions. After Lys_{18} was added to 50 μM and the solution was mixed briefly, the sample turned opaque immediately (top row, middle), due to the formation of actin bundles. When examined through crossed polarizers, the sample no longer appeared to be birefringent (bottom row, middle). This result suggests that the formation of bundles disrupted the long range liquid crystalline order in the initial F-actin solution. When 10 mM ATP, which disaggregates cation-induced actin bundles (*11*), was added, the solution became transparent (top row, right), and the nematic order was restored, as judged by the reappearance of a birefringence pattern (bottom row, right). Note that the liquid crystalline order is not a prerequisite for bundle formation, and all the light scattering measurements reported here were carried out on initially isotropic suspensions.

Ionic Strength and Filament Concentration Have Opposite Effects on F-Actin Bundles Induced by Polycations and by Polyethylene Glycol. In contrast to liquid crystalline formation, steric exclusion (*40*, *41*) of filamentous biopolymers by inert solutes such as polyethylene glycol (PEG) can facilitate the formation of lateral aggregates that are morphologically similar to the cation-induced bundles (*22*, *42*). The PEG-induced bundling is experimentally manifested in different features from the cation-induced bundle formation. For instance, in the latter case, an increase in the concentration of the macromolecules will require more polyvalent cations to induce the bundle formation (*10*, *11*), while less PEG is required to cause bundle formation by filaments at a higher concentration (*22*), corresponding to a larger total excluded volume.

The two classes of bundling phenomena also exhibit an opposite dependence on ionic strength. Figure 6a shows by low-speed sedimentation that F-actin at 0.5 mg/mL is induced to bundle by a well-defined weight percentage of PEG-6000, and the percentage decreases monotonically with the concentration of KCl in solution. Figure 6b compares the onset concentrations of PEG-6000 and lysozyme required to induce actin bundle formation as a function of solution ionic strength. The PEG data in open symbols are derived from Figure 6a. Each value of the PEG concentration at a specific KCl concentration corresponds to the onset of a steep increase in the low-speed pellet. The lysozyme data are derived similarly from the respective data curves in Figure 1. The decrease in the concentration of PEG-6000 required to bundle F-actin with the increase in KCl concentration suggests in this case that simple charge screening plays a dominant role, and the filaments are more easily driven

together when screened more efficiently at a higher ionic strength. The opposite dependence on ionic strength in the case of lysozyme-induced bundling is due to the competition in binding between monovalent and polyvalent cations. A similar property for the polylysine-induced bundle formation has been demonstrated in Figure 4.

DISCUSSION

The formation of bonds between proteins in their native state generally depends on complementary surfaces on each protein that permit specific bonds between individual atoms on each polypeptide. Such sites depend on both the amino acid sequence and the secondary and tertiary structure that allow appropriate juxtaposition of binding sites. As a result, the number of physiologically significant protein−protein interactions is thought to be small for a typical protein, and this expectation is basic with respect to using such methods as affinity chromatography or two-hybrid screens to identify binding partners. In contrast to this general rule for individual polypeptides or even multisubunit protein complexes, filamentous protein polymers such as the elements of the cytoskeleton appear to have dozens or perhaps hundreds of ligands in vivo. F-Actin is perhaps the most striking example for such a multiplicity. The large number of proteins that bind specifically F-actin, compared to the much smaller number of proteins that bind G-actin, is paradoxical when considered in relation to the much smaller surface available on each F-actin subunit, since much of its surface is buried in the multiple actin−actin bonds holding the filament together. The multitude of F-actin binding proteins suggests that physicochemical interactions in addition to those traditionally considered in the formation of stereospecific protein−protein bonds may be important for the function of proteins that bind specifically to filamentous protein polymers.

One significant difference between protein filaments and individual proteins or oligomeric complexes is the fact that the former can have properties of polyelectrolytes in solution, and the latter cannot, simply because they are too small (*4*, *43*). Each of the three cytoskeletal filament types, as well as many filamentous viruses, has negative electrostatic surface charge densities similar to those of DNA, for which theories of polyelectrolyte effects are well-developed and consistent with experimental results. The binding of cationic ligands to anionic filaments has been shown in the case of DNA to be stabilized in part by the electrostatic attraction between the binding pair, and perhaps more importantly by the entropy gained by the release of mono- or divalent cations condensed on the polyelectrolyte when a multivalent ligand binds to the filament (*44*, *45*). The work presented here was undertaken to evaluate the extent to which electrostatic effects contribute to the binding of cationic proteins to a variety of anionic protein-based filaments using filament bundle formation as a measure of effective binding.

In the case of F-actin bundle formation, the bundling agent has been thought to require at least two separate specific actin binding sites in order to directly bridge two parallel actin filaments. While several actin bundling proteins fulfill this requirement, others apparently do not, and the functions of such proteins appear to be described by the electrostatic model proposed here. The polyelectrolyte nature of F-actin makes it prone to association with proteins or other ligands carrying a few positive charges. Such an interaction may enhance the hydrophobicity of the total ligand−substrate complex due to neutralization of the charged residues. Consequently, further aggregation may occur, and at appropriate conditions, paracrystalline actin bundles are formed.

Our results show several general features common to bundling of distinct filaments. Figure 1 shows that a number of structurally unrelated proteins and peptides can induce the formation of actin bundles with efficiencies similar or greater than those of physiologically important bundling factors such as fimbrin or villin. One of the actin bundling proteins, calponin, has previously been shown to bind actin in a manner at least partly dependent on electrostatics (*34*) and to possess only one specific actin binding site (*46*, *47*). One prediction of the electrostatic model proposed here is that binding and bundling activities may not be unique to a particular filamentous ligand. This expectation is borne out in Figure 2 which shows efficient ATP-dependent bundling of vimentin intermediate filaments by calponin under conditions similar to those required for bundling F-actin. This result may have physiologic significance since a protein isolated from smooth muscle as an ATP-dependent bundling factor of the vimentin homologue desmin appears to be similar to or identical with calponin (*48*), and more recently, direct interaction of purified calponin and desmin intermediate filaments has been shown (*49*, *50*). The generality of cation-induced filament bundling is further demonstrated in Figure 3 by the ability of lysine oligomers to bundle six structurally distinct anionic filaments with efficiencies that are at least qualitatively related to the polyelectrolyte surface charge.

The mechanism by which polyvalent cations induce filament bundles is different from the bundling of filaments by inert solutes such as polyethylene glycol (PEG). The phenomenon of PEG-induced aggregation of F-actin is related to the effects of PEG on protein solubility (*40*, *41*, *51*, *52*) due primarily to the effect of steric exclusion, or preferential hydration, in the sense that there is a layer near the protein surface from which PEG is excluded but water is not. With increasing concentrations of PEG, such exclusion effects make it unfavorable for the protein molecules to be surrounded by the solvent, and precipitation of protein occurs at a threshold concentration of PEG. This model of steric exclusion has also been successfully applied to filamentous biopolymers such as microtubules (*51*) and F-actin (*22*, *42*). In the case of DNA, PEG-induced condensation has been studied in detail by X-ray in order to determine the interfilament spacing as a function of PEG concentration (*53*). An alternative thermodynamic treatment of these data has been presented by Ito et al. (*54*).

It is interesting to note that the PEG-induced protein precipitation can also be explained by the concept of depletion flocculation, widely known to colloidal scientists (*55*, *56*). Asakura and Oosawa showed (*57*, *58*) that an effectively attractive interaction between two noninteracting macromolecules can be induced by inert polymers in solution. The attractive force increases with the concentration of inert polymers, and it is stronger in solutions of macromolecules with an asymmetrical shape than that between spherical macromolecules (*58*). These predictions explain well the phenomenon of PEG-induced protein precipitation, especially the bundle formation of the asymmetrical actin filaments in the presence of PEG. The thermodynamic origin of such a

phenomenon is steric exclusion, and the same concept was later formulated differently (*40*, *41*, *51*, *52*). The latter model has been widely accepted among biochemists and is therefore adopted in this paper.

The mechanism of liquid crystalline formation of F-actin is different from bundle formation (Figure 5). Liquid crystalline formation is entropy-driven. An increase in the concentration of F-actin decreases the entropy of an isotropic distribution more than that of the filaments aligned into parallel arrays. Therefore, the liquid crystalline phase appears above a well-defined threshold concentration of actin. The threshold concentration is found to be nearly unaffected by the χ parameter which characterizes the solvent−solute interaction (*59*), until such a transition is disturbed by the onset of bundle formation (*22*). A typical phase diagram such as that presented in Suzuki et al. (*22*) can also be found for spermidine-condensed DNA (*60*), and for stiff chain polymers such as poly(γ-benzyl-L-glutamate) (*61*). However, in the case of spermidine-condensed DNA, a net attractive interaction exists between the neighboring DNA molecules, which is mediated by the polyvalent cations. Therefore, in contrast to the PEG-induced bundle formation, the similar phase diagram actually arises from very different interactions as illustrated in this work.

Herzfeld and co-workers have recently published a series of papers aimed at predicting the organization of cytoskeletal elements (*62*−*65*). The prediction of their model generally agrees with the experimental observations of both the isotropic−liquid crystalline transition of F-actin alone and the bundle formation of F-actin induced by PEG (*64*). In their model, only repulsive interactions are assumed between the neighboring filaments; hence, their treatment does not include the effect of polycations or cross-linking proteins on bundle formation.

Since over 30% of a typical cell volume is occupied by macromolecules such as DNA, RNA, proteins, and polysaccharides (*66*), a general term "macromolecular crowding" has been designated to address two large classes of phenomena in cells (*62*, *67*−*70*). The thermodynamic origin of macromolecular crowding is the excluded volume effect favoring a compact molecular conformation (*70*), spontaneous alignment of filamentous particles at high concentrations (*36*), and the segregation of solute molecules with disparate sizes and geometries (*62*−*64*). Protein precipitation by inert polymers has been thought to be due to the effect of steric exclusion (*40*, *41*). A second class of macromolecular crowding effects includes increased ligand−substrate binding and enhancement in any biochemical activities under crowded conditions (*69*, *70*). For instance, in the case of actin bundle formation, lower concentrations of polycations, cationic proteins, or other cross-linking proteins are required when the F-actin solution is crowded by an inert polymer such as PEG-6000 (*67*).

Bundle formation by F-actin and other cytoskeletal filaments plays important roles in cell functions. While some bundles of F-actin such as stress fibers are relatively stable, other structures such as filopodia are more transient. Both formations are strongly affected by various binding proteins and changes in ionic conditions, including pH, free Ca^{2+} and Mg^{2+} concentrations, and the level of anionic phosphates such as ATP. Contributions from the rather general effects illustrated in this paper may be important for their formation and dissolution and the activation of specific bundling proteins. For instance, depletion of ATP following cellular oxidant injury has been shown to be accompanied by the occurrence of side-to-side aggregates or bundles of microfilaments (*71*). Such an observation can partly be explained as being due to activation of cationic actin bundling factors which were sequestered by the polyanionic ATP prior to its depletion. In conclusion, detailed analysis of the mechanisms and experimental features illustrated in this paper provides a conceptual framework with which to understand a large class of interactions between the cytoskeleton and subcellular ionic components in the crowded environment of the cytoplasm.

ACKNOWLEDGMENT

We thank Phong T. Tran for the gift of tubulin and Bing Li for preparation of calponin. The discussion referring to depletion flocculation was kindly suggested to us by Professor Seth Fraden of Brandeis University. We also thank Jagesh V. Shah for a critical reading and other members of the Experimental Medicine Division for ongoing assistance.

REFERENCES

1. Alberts, B., Bray, D., Lewis, J., Raff, M., Roberts, K., and Watson, J. (1994) *Molecular biology of the cell*, 3rd ed., Garland, New York.
2. Bloomfield, V. A. (1991) *Biopolymers 31*, 1471−1481.
3. Marquet, R., and Houssier, C. (1991) *J. Biomol. Struct. Dynam. 9*, 159−167.
4. Manning, G. S. (1978) *Q. Rev. Biophys. 11*, 179−246.
5. Oosawa, F. (1971) *Polyelectrolytes*, pp 113, Marcel Dekker, Inc., New York.
6. Ray, J., and Manning, G. S. (1994) *Langmuir 10*, 2450−2461.
7. Israelachvili, J. (1992) *Intermolecular & Surface Forces*, 2nd ed., pp 83−108, Academic Press, New York.
8. Israelachvili, J., and Wennerstrom, H. (1996) *Nature 379*, 219−225.
9. Rau, D. C., and Parsegian, V. A. (1990) *Science 249*, 1278−1281.
10. Tang, J. X., Wong, S., Tran, P. T., and Janmey, P. A. (1996) *Ber. Bunsen-Ges. Phys. Chem. 100*, 796−806.
11. Tang, J. X., and Janmey, P. A. (1996) *J. Biol. Chem. 271*, 8556−8563.
12. Fowler, W. E., and Aebi, U. (1982) *J. Cell Biol. 93*, 452−458.
13. Grant, N. J., Oriol-Audit, C., and Dickens, M. J. (1983) *Eur. J. Cell Biol. 30*, 67−73.
14. Kawamura, M., and Maruyama, K. (1970) *J. Biochem. (Tokyo) 68*, 885−899.
15. Owen, C. H., DeRosier, D. J., and Condeelis, J. (1992) *J. Struct. Biol. 109*, 248−254.
16. Stokes, D. L., and DeRosier, D. J. (1991) *Biophys. J. 59*, 456−465.
17. Schmid, M. F., Matsudaira, P., Jeng, T.-W., et al. (1991) *J. Mol. Biol. 221*, 711−725.
18. Coppin, C., and Leavis, P. (1992) *Biophys. J. 63*, 794−807.
19. Furukawa, R., Kundra, R., and Fechheimer, M. (1993) *Biochemistry 32*, 12346−12352.
20. Käs, J., Strey, H., Tang, J. X., et al. (1996) *Biophys. J. 70*, 609−625.
21. Suzuki, A., Maeda, T., and Ito, T. (1991) *Biophys. J. 59*, 25−30.
22. Suzuki, A., Yamazaki, M., and Ito, T. (1996) *Biochemistry 35*, 5238−5244.
23. Spudich, J., and Watt, S. (1971) *J. Biol. Chem. 246*, 4866−4871.
24. Gong, B.-J., Mabuchi, K., Takahashi, K., Nadal-Ginard, B., and Tao, T. (1993) *J. Biochem. 114*, 453−456.
25. Voter, W. A., and Erickson, H. P. (1984) *J. Biol. Chem. 256*, 10430−10438.

26. Nelson, W. J., and Traub, P. (1982) *J. Biol. Chem. 257*, 5536−5543.
27. Caspar, D. L. D. (1963) *Adv. Protein Chem. 18*, 37.
28. Sambrook, J., Fritsch, E. F., and Maniatis, T. (1989) *Molecular Cloning: A Laboratory Manual*, 2nd ed., pp 4.21−4.32, Cold Spring Harbor Laboratory Press, Plainview, NY.
29. Maniotis, A. J., Chen, C. S., and Ingber, D. E. (1997) *Proc. Natl. Acad. Sci. U.S.A. 94*, 849−854.
30. Svitkina, T. M., Verkhovsky, A. B., and Borisy, G. G. (1996) *J. Cell Biol. 135*, 991−1007.
31. Pedrotti, B., Colombo, R., and Islam, K. (1994) *Biochemistry 33*, 8798−8806.
32. Itano, N., and Hatano, S. (1991) *Cell Motil. Cytoskeleton 19*, 244−254.
33. Kolakowski, J., Makuch, R., Stepkowski, D., and Dabrowska, R. (1995) *Biochem. J. 306*, 199−204.
34. Tang, J. X., Szymanski, P., Janmey, P. A., and Tao, T. (1997) *Eur. J. Biochem. 247*, 432−440.
35. Zimmermann, K., Hagedorn, H., Heuck, C. C., Hinrichsen, M., and Ludwig, H. (1986) *J. Biol. Chem. 261*, 1653−1655.
36. Onsager, L. (1949) *Ann. N.Y. Acad. Sci. 51*, 627−659.
37. Odijk, T. (1986) *Macromolecules 19*, 2313−2329.
38. Tang, J. X., and Fraden, S. (1995) *Liq. Cryst. 19*, 459−467.
39. Stroobants, A., Lekkerkerker, H. N. M., and Odijk, T. (1986) *Macromolecules 19*, 2232−2238.
40. Arakawa, T., and Timasheff, S. N. (1985) *Biochemistry 24*, 6756−6762.
41. Bhat, R., and Timasheff, S. N. (1992) *Protein Sci. 1*, 1133−1143.
42. Suzuki, A., Yamazaki, M., and Ito, T. (1989) *Biochemistry 28*, 6513−6518.
43. Zhang, W., Bond, J. P., Anderson, C. F., Lohman, T. M., and Record, M. J. (1996) *Proc. Natl. Acad. Sci. U.S.A. 93*, 2511−2516.
44. Anderson, C. F., and Record, M. J. (1990) *Annu. Rev. Biophys. Biophys. Chem. 19*, 423−465.
45. Anderson, C. F., and Record, M. J. (1995) *Annu. Rev. Phys. Chem. 46*, 657−700.
46. Mezgueldi, M., Mendre, C., Calas, B., Kassab, R., and Fattoum, A. (1995) *J. Biol. Chem. 270*, 8867−8876.
47. Mezgueldi, M., Fattoum, A., Derancourt, J., and Kassab, R. (1992) *J. Biol. Chem. 267*, 15943−15951.
48. Nakagawa, H., Ishihara, M., and Ohashi, K. (1993) *J. Biochem. (Tokyo) 114*, 623−626.
49. Mabuchi, K., Li, B., Ip, W., and Tao, T. (1997) *J. Biol. Chem. 272*, 22662−22666.
50. Wang, P., and Gusev, N. B. (1996) *FEBS Lett. 392*, 255−258.
51. Lee, J. C., and Lee, L. L. Y. (1979) *Biochemistry 18*, 5518−5526.
52. Lee, J. C., and Lee, L. L. Y. (1981) *J. Biol. Chem. 256*, 625−631.
53. Rau, D. C., Lee, B., and Parsegian, V. A. (1984) *Proc. Natl. Acad. Sci. U.S.A. 81*, 2621−2625.
54. Ito, T., Yamazaki, M., and Ohnishi, S. (1989) *Biochemistry 28*, 5626−5630.
55. Hunter, R. J. (1987) *Foundations of Colliod Science*, pp 483−485, Clarendon Press, Oxford.
56. Lowen, H. (1997) *Phys. A 235*, 129−141.
57. Asakura, S., and Oosawa, F. (1954) *J. Chem. Phys. 22*, 1255−1256.
58. Asakura, S., and Oosawa, F. (1958) *J. Polym. Sci. 33*, 183−192.
59. Flory, P. J. (1978) *Principles of Polymer Chemistry*, pp 495−539, Cornell University Press, London.
60. Sikorav, J.-L., Pelta, J., and Livolant, F. (1994) *Biophys. J. 67*, 1387−1392.
61. Miller, W. G. (1978) *Annu. Rev. Phys. Chem. 35*, 519−535.
62. Herzfeld, J. (1996) *Acc. Chem. Res. 29*, 31−37.
63. Kulp, D. T., and Herzfeld, J. (1995) *Biophys. Chem. 57*, 93−102.
64. Madden, T. L., and Herzfeld, J. (1993) *Biophys. J. 65*, 1147−1154.
65. Madden, T. L., and Herzfeld, J. (1996) *J. Cell Biol. 126*, 169−174.
66. Zimmerman, S. B., and Trach, S. O. (1991) *J. Mol. Biol. 222*, 599−620.
67. Cuneo, P., Magri, E., Verzola, A., and Grazi, E. (1992) *Biochem. J. 281*, 501−512.
68. Walter, H., and Brooks, D. E. (1995) *FEBS Lett. 361*, 135−139.
69. Zimmerman, S. B., and Minton, A. P. (1993) *Annu. Rev. Biophys. Biomol. Struct. 22*, 27−65.
70. Zimmerman, S. B., and Murphy, L. D. (1996) *FEBS Lett. 390*, 245−248.
71. Hinshaw, D. B., Armstrong, B. C., Burger, J. M., Beals, T. F., and Hyslop, P. A. (1988) *Aust. J. Pharm. 132*, 479−488.

BI9711386